High-Pressure Studies of Dynamic Solvent Effects on Large Amplitude Isomerization: 2-(2-Propenyl)anthracene

Kimihiko Hara,* Naoki Ito, and Okitsugu Kajimoto

Division of Chemistry, Graduate School of Science, Kyoto University, Sakyo-ku, Kyoto 606-01 Japan

Received: September 24, 1996; In Final Form: December 20, 1996[⊗]

Effect of pressure on the excited-state isomerization rate of 2-(2-propenyl)anthracene in a series of alkane solvents was examined by steady-state and picosecond time-resolved fluorescence spectroscopy. The viscosity dependence of the isomerization rate constant was analyzed by the theories of the dynamic solvent effect on chemical reactions. The viscosity dependence is sufficiently smaller than that predicted by Kramers theory. The experimental result was analyzed by the frequency-dependent friction defined in the Grote−Hynes theory, and the barrier top frequency ($\omega_b = 9.6 \times 10^{12}$ s^{-1}) was determined.

Introduction

Understanding how chemical reactions in solution are affected by solvent dynamical motion is a topic of recent interest in physical chemistry.[1] Isomerization reactions in solution usually involve large amplitude motion of a bulky group twisting around a molecular axis. Therefore, the twisting motion will experience the effect of frictional forces exerted by the surrounding solvent molecules.

The excited-state isomerization of 2-alkenylanthracene is a reaction that is well suited for the purpose of studying the dynamic solvent effect on isomerization.[2−5] This isomerization has a nondipolar transition state, which proceeds in nonpolar solvents. It can be described as crossing over a simple one-dimensional potential barrier amenable to theoretical analysis. The reaction coordinate is envisaged as a torsional motion about the single bond that connects the anthracene ring and the alkenyl group, which is referred to as *s-cis* ⇔ *s-trans* isomerization in the lowest excited singlet (S_1) state,

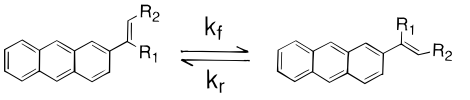

(1)

Furthermore, it should be noted that the barrier crossing rate of the 2-alkenylanthracene isomerization in the S_1 state is much more rapid compared to the $S_1 \rightarrow S_0$ deactivation rate so that this can be treated as a pure S_1 state isomerization where the emission from both conformers are detectable. This is in contrast with the S_1 state isomerization of diphenylpolyenes such as *trans*-stilbene and 1,4-diphenylbutadiene (DPB), in which the fast deactivation ocurrs from the intermediate "phantom state"[6] having a planar configuration and a zwitterionic character.[7]

Previously, we have investigated the dynamic solvent effect on the S_1-state isomerization of 2-vinylanthracene (2VA) (R_1═H, R_2═H) by using high-pressure picosecond laser spectroscopy.[8] High-pressure provides a large viscosity change in a *single* solvent without modifying the solvent-shell structure in any sizable amount. The molecule adopted in this study is 2-(2-propenyl)anthracene (22PA) (R_1═CH_3, R_2═H), which possesses a larger twisting moiety than 2VA.

This paper describes the high-pressure research on the S_1-state isomerization of 22PA in a series of *n*-alkane solvents over a wide range of solvent viscosity and also gives a discussion of the dynamic solvent effect in comparison with the previous results of 2VA.[8,9]

Experimental Section

22PA was synthesized using the method of Stolka et al.[10] and was purified by thin layer chromatography (TLC). The liquid *n*-alkanes (*n*-pentane, *n*-hexane, *n*-octane, and *n*-decane) employed as solvents were spectroscopic grade, which were checked for background fluorescence. The liquid sample solutions used in the measurements of steady-state and time-resolved fluorescence spectra were degassed by repeated freeze−pump−thaw cycles just before use. The measurements were performed for solutions with a concentration of $\sim 10^{-5}$ M at 303 K as a function of pressure up to 490 MPa. A high-pressure optical cell equipped with four sapphire windows was used, which was described previously.[11]

Picosecond time-resolved fluorescence spectra at high pressures were measured by the method of time-correlated single-photon counting (TCSPC). The experimental arrangement of the laser system was reported previously.[12] The second harmonic radiation of a mode-locked Ti:sapphire laser (Spectra-Physics, Tsunami Model 3950) was used as the excitation light source. The excitation wavelength was 375 nm, where the A conformer is excited dominantly. The Ti:sapphire laser, which was pumped by a CW argon ion laser, produces 730−960 nm light pulses of 1.5 ps duration and has a repetition rate of 82 MHz. The pulse repetition rate was decreased to 8.2 MHz by using an electro-optic light modulator (Con Optic, Model 1305). A Hamamatsu R2809-02u microchannel plate (MCP) photomultiplier tube was used for detection.

The overall instrument response function has an fwhm of approximately 30 ps at the detection wavelength. Data were stored in a computer (NEC PC 9801) equipped with a multichannel analyzing (MCA) system. The transient data are fit with sums of functions that are convoluted with the instrument response function. The iterative nonlinear least-squares algorithm was performed on an Epson PC-486GR computer. Data were collected until $\sim 10^4$ counts were accumulated in the peak channel. The precision of the fluorescence lifetime is estimated as ∼5%.

* To whom correspondence should be addressed (e-mail hara@kuchem.kyoto-u.ac.jp).

[⊗] Abstract published in *Advance ACS Abstracts,* February 15, 1997.

S1089-5639(96)02941-6 CCC: $14.00

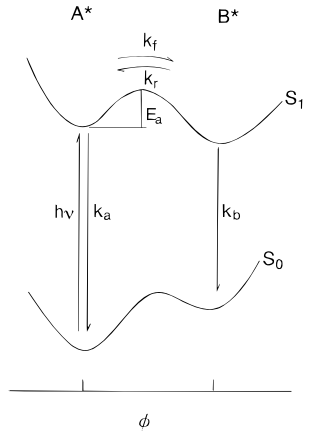

Figure 1. Potential energy diagram of the ground (S_0) and lowest excited singlet (S_1) state of alkenylanthracene indicated as a function of twisting angle (ϕ) between the alkane and anthracene planes.

Kinetic Analysis

The potential profile of the S_1 state isomerization of 22PA is illustrated in Figure 1. The reaction coordinate is envisaged along the dihedral angle (ϕ), indicating the torsional motion about the single bond that connects the anthracene ring and the propenyl group. It should be noted that the *s-cis* form is tentatively referred to as A conformer, while the *s-trans* form is referred to as B conformer, since the geometrical identification has not been unequivocally established experimentally and theoretically.

When the photophysical rate equations in the framework of the scheme illustrated in Figure 1 are solved, the expression for the emission intensity $I(t)$ is obtained. It provides that the emission dynamics should be biexponentials with two time constants. By assuming that the deactivation rates from the S_1- to the S_0-state for both conformers are equal ($k_a = k_b$), the forward rate constant (k_f) of the isomerization is reduced to the following relation:[3,8]

$$k_f = (\tau_1^{-1} - \tau_2^{-1})/(1 + 1/K^*) \qquad (2)$$

where τ_1 and τ_2 are the fast and slow time constants, respectively. K^* is the S_1-state equilibrium constant expressed by the ratio of the forward to reverse rate constant ($=k_f/k_r$). The derivation of eq 2 has been described in detail previously.[3,8] As a consequence, determining the value of K^* by the steady-state measurement and the values of two time constants (τ_1, τ_2) by the time-resolved measurement, we can obtain the k_f value by applying eq 2.

Results

Static Spectroscopy. Representative steady-state fluorescence spectra of 22PA in *n*-pentane at 0.1 and 490 MPa at 303 K are illustrated in Figure 2. The observed spectra were simulated by assuming that they are composed of the overlapping of A* and B* emission spectra. Four fundamental vibrational bands corresponding to the anthracene moiety, i.e., (0_0^0), (12_1^0), (6_1^0) and (6_2^0), were taken into consideration for each simulation of A* and B* emission spectra. A Gaussian form was supposed for each of the vibrational bands. In Figure 2 the separated A* and B* emission spectra and reproduced emission spectra are included. The K^* value was determined as the averaged value of the area ratios of B* to A* vibronic emission bands. The K^* values thus resulted are slightly decreased with increasing solvent shear viscosity (η), ranged around 3.0−2.5 for pressures up to 490 MPa, whose aspect is shown in Figure 3.

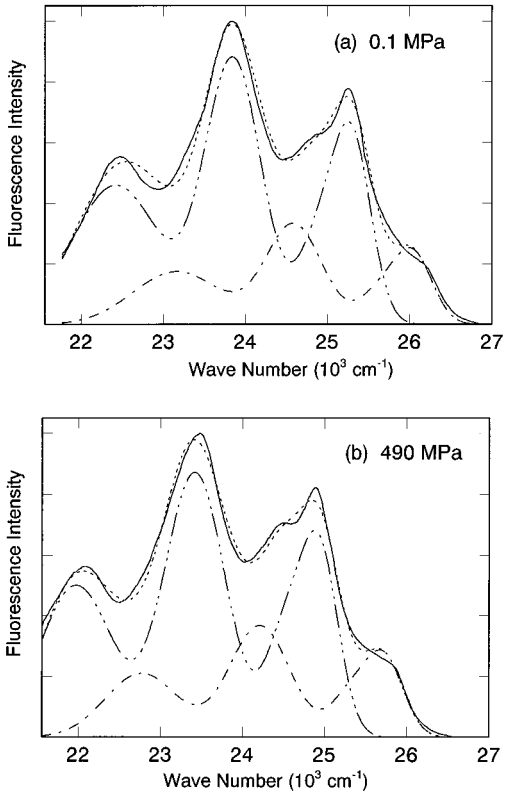

Figure 2. Examples of observed (—) and simulated (- - -) fluorescence spectra of 22PA in *n*-pentane at 303 K: (a) 0.1 MPa; (b) 490 MPa. The separated spectra of A* (— - —) and B* (— - -) are included.

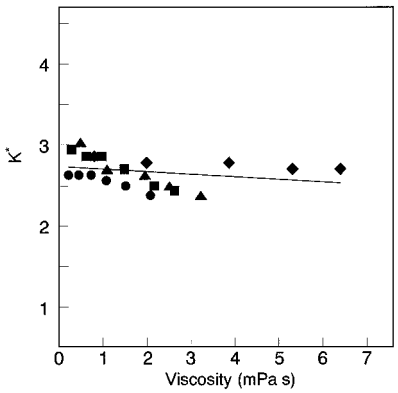

Figure 3. Plot of K^* as a function of solvent viscosity in compressed alkanes: (●) *n*-pentane; (■) *n*-hexane; (▲) *n*-octane; (◆) *n*-decane.

Dynamic Spectroscopy. Upon the selective excitation of the A conformer at the wavelength of 375 nm, the time dependence of the fluorescence intensity ($I(t)$) detected at both A* and B* emission wavelengths is reasonably represented by a simple biexponential form:

$$I(t) = A_1 \exp(-t/\tau_1) + A_2 \exp(-t/\tau_2) \qquad (3)$$

with a short time constant (τ_1) and a long time constant (τ_2). Here, A_1 and A_2 are the pre-exponential terms containing the rate constants of each photoelementary process. Representative fluorescence response curves are shown in Figure 4. The solid lines running through the data points represent the fittings to eq 3. When monitored at the wavelength of A* emission, $I(t)$ exhibits two decaying exponentials, indicating that both A_1 and A_2 are positive. When monitored at the wavelength of B* emission, $I(t)$ exhibits one decaying and one rising exponential,

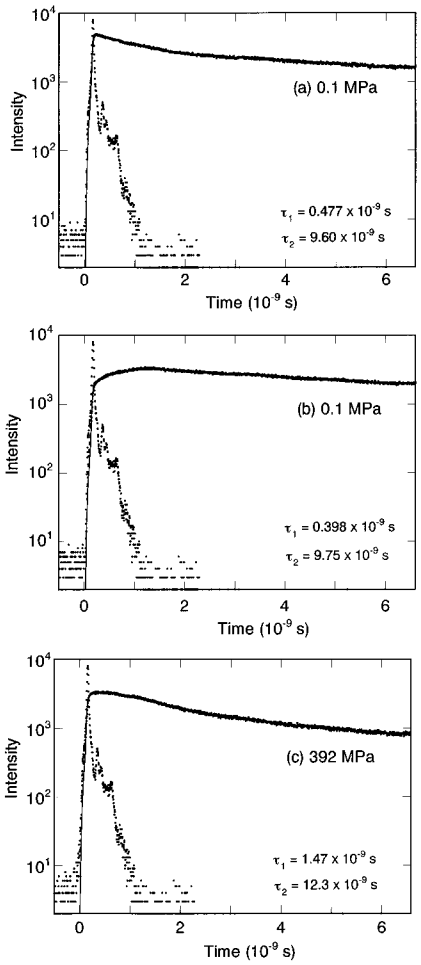

Figure 4. Representative fluorescence response curves of 22PA in *n*-hexane at 303 K: (a) at 0.1 MPa monitored at A* emission wavelength (383.5 nm); (b) at 0.1 MPa monitored at B* emission wavelength (397 nm); (c) at 490 MPa monitored at A* emission wavelength (388 nm).

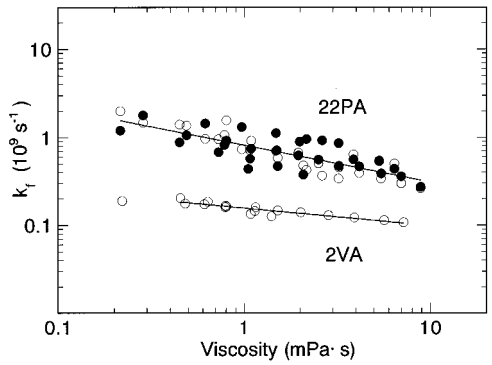

Figure 5. Plot of ln k_f against ln η for 22PA: (○) monitored at A* emission; (●) monitored at B* emission. The result of 2VA[8] is shown for comparison.

indicating that A_1 is negative and A_2 is positive. The τ values are independent of excitation wavelength. In addition, the fact that the experimental response function are well reproduced by the biexponential formula (eq 3) demonstrates that the model of two stable states depicted in Figure 1 is reasonably applicable to this isomerization.

Viscosity Dependence of k_f. In Figure 5, the resulting k_f values were plotted as a function of solvent shear viscosity (η) in double logarithmic scale. The high-pressure η values for *n*-alkanes were obtained from extrapolation or interpolation of literature data[13] by using a third-order polynomial relation.[14] The viscosity examined covers the range 0.215−8.84 mPa s. This figure contains the k_f values of four compressed alkanes from *n*-pentane to *n*-decane, which are monitored at both A* and B* emission wavelengths. The errors in k_f values mostly originated from the deviation in the zero-time determination in the deconvolution process. The η dependence of k_f shows a monotonic decreasing behavior irrespective of solvents. This result substantiates that the reaction kinetics is in the *spatial diffusion*-controlled regime. We fit k_f to η using the empirical power-law formula representing the fractional power dependence of rate on viscosity:

$$k_f = A\eta^{-\alpha} \tag{4}$$

where A is the viscosity-independent constant. The exponent α is used as a measure of solvent viscosity dependence. In Figure 5 the previous result of 2VA is included for comparison.

When we determine the α value by the high-pressure method, the intrinsic pressure dependence on the reaction rate should be taken into consideration; i.e., the apparent rate constant can be written as

$$k_f = A'\eta^{-\alpha}k_{TST} \tag{5}$$

where k_{TST} is the rate constant defined by transition-state theory (TST). For the case of isomerization with a one-dimensional double-well potential, k_{TST} is reduced to

$$k_{TST} = (\omega_0/(2\pi))\exp(-E_a/(RT)) \tag{6}$$

where ω_0 is the frequency corresponding to the curvature of the reactant well considered as a parabola and E_a is the barrier energy. By differentiating eq 5 with respect to pressure, we obtain

$$\alpha = -(\partial \ln k_f/\partial \ln \eta) - (\Delta V^{\ddagger}_{TST}/(RT))/(\partial \ln \eta/\partial P) \tag{7}$$

where $\Delta V^{\ddagger}_{TST}$ is the activation volume defined by $-RT(\partial \ln k_{TST}/\partial P)$.

For liquid alkanes from *n*-pentane to *n*-decane, the value of $(\partial \ln \eta/\partial P)$ is in the range $(8.5-11.5) \times 10^{-9}$ Pa^{-1}. Whereas the value of $|\Delta V^{\ddagger}_{TST}|$ is estimated to be less than 0.5 cm^3/mol for the isomerization as in the present case.[8,15] It follows that the second term in eq 7, $(\Delta V^{\ddagger}_{TST}/(RT))/(\partial \ln \eta/\partial P)$ amounts to 0.023−0.017, which is approximately 5% of the first term in eq 7. Therefore, it is concluded that the α value can be determined only from the first term within the present experimental errors.

The α value thus obtained from the fitting to the power law relation is 0.40 ± 0.02, which is appreciably larger than that of 2VA ($\alpha = 0.20$). The difference in the viscosity dependence between 22PA and 2VA can be understood by the larger size of the rotating group in 22PA. In addition, for both 22PA and 2VA, it is concluded that the viscosity dependence is much weaker than that predicted from the Kramers theory ($\alpha = 1$).[16] In Table 1 the present α value is compared to previous results and those of *trans*-stilbene and DPB. Barbara and co-workers[2] have presented much smaller α values, that is, 0.2 for 22PA and ∼0 for 2VA, by measuring in a series of different solvents, which covers 0.2−3.5 mPa s. It should be stressed here that the more reliable result could be obtained by the high-pressure study, which makes it possible to cover the wider viscosity range without variation of activation energy.

Discussion

Calculation of Frequency-Dependent Friction. To understand such weak viscosity dependence, which indicates the

TABLE 1: Barrier Crossing Parameters of Excited Isomerizations, Power-Law Parameter (α), Barrier Frequency (ω_b), and Barrier Energy (E_a)

	α	ω_b 10^{12} s^{-1}	E_a kJ/mol	ref
22PA	0.40	9.6		this work
	0.23	8.9	15.5	5
2VA	0.20	11.4		9
	∼0	15.6	22.2	3, 5
trans-stilbene	0.32	1.5	14.6	18
DPB[a]	0.59	6.0	19.7	24

[a] 1,4-Diphenylbutadiene.

TABLE 2: Density (ρ), Sound Velocity (c), Zero-Frequency Shear Viscosity (η), and Zero-Frequency Bulk Viscosity (η_v) of *n*-Hexane, Which Are Used for the Calculation of Frequency-Dependent Friction[20,21]

pressure (MPa)	ρ (kg/m^3)	c (m/s)	η (mPa s)	η_v (mPa s)
0.1	650	1060	0.293	1.708
49.1	697	1365	0.497	2.278
98.1	721	1584	0.63	3.138
196.1	760	1903	1.107	4.013
392.3	810	2310	2.4	5.905

breakdown of the Kramers theory,[16] the idea of frequency-dependent friction originally introduced by Grote and Hynes[17] has often been employed alternatively.[1] The assumption of the Kramers theory breaks down when the transit time over the barrier is comparable with the time between collisions of solute with solvent. In the model of Grote and Hynes,[17] the correlation between random forces of the solvent is taken into account through a frequency-dependent friction. The motion of the particle representing the isomerizing molecule is determined by a generalized Langevin equation. It follows that the viscosity dependence is weaker than the η^{-1} that would be expected by the Kramers theory.

In the Grote−Hynes (G−H) theory,[17] the apparent rate constant for parabolic barrier crossing is then given by

$$k = (\lambda_r/\omega_b)k_{TST} \tag{8}$$

The ratio $(\lambda_r/\omega_b) = \kappa$ is the dynamical transmission coefficient describing the reduction of k below the TST value. Here ω_b is the frequency describing the parabolic top of the potential barrier. The reactive frequency (λ_r) is determined by the following self-consistent relation:

$$\lambda_r = (\omega_b)^2/[\lambda_r + \hat{\zeta}(\lambda_r)/I] \tag{9}$$

where I is the moment of inertia of the isomerizing group. Note that eq 9 involves the barrier frequency (ω_b) and the Laplace transform frequency component of the friction:

$$\hat{\zeta}(\lambda_r) = \int_0^\infty \exp(-\lambda_r t)\zeta(t)\, dt \tag{10}$$

This depends on the details of the isomerization, such as the size of the isomerizing group.

The frequency-dependent friction ($\hat{\zeta}(\lambda_r)$) was calculated for the S_1-state 22PA isomerization in *n*-hexane. The method of computation is the same as reported previously[9,18,19] in which the isomerization is modeled as a rotation around a fixed axis of two spheres of hydrodynamic radius (d), which are separated from the axis by a distance (r). A slip boundary condition is supposed to be valid. In this case, there is no rotational friction.

Various physical constants of the solvent are needed in order to compare the frequency-dependent friction model with the experimental frequency factor. The high-pressure values of zero-frequency shear viscosity (η), zero-frequency bulk viscosity (η_v), sound velocity (c), and density (ρ) can be obtained only for *n*-hexane.[20,21] The quantities used for the numerical calculation are listed in Table 2.

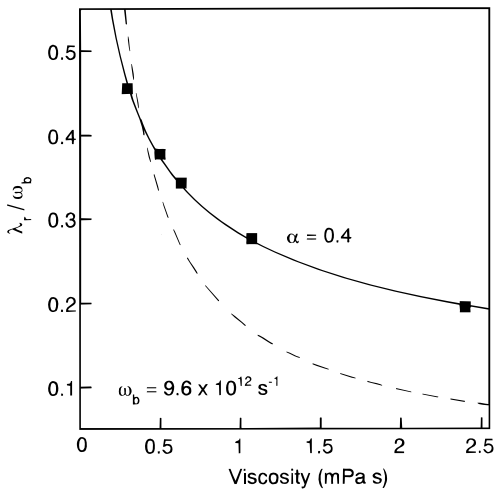

Figure 6. Plot of transmission coefficient λ_r/ω_b as a function of solvent sheaviscosity (η) for 22PA in *n*-hexane: (■) calculated points; (−) line representing $\lambda_r/\omega_b = A\eta^{-0.40}$; (- - -) result from Kramers theory shown for comparison.

A least-squares fitting of eqs 8 and 9 to the experimental viscosity dependence of the isomerization rate constant was performed by varying the ω_b value as a parameter. The optimal value of $\omega_b = 9.6 \times 10^{12}$ s^{-1} was determined with a bulk modulus $K_r = 10^9$ N/m^2 and a shear modulus $G_\infty = 10^9$ N/m^2.[19] Figure 6 illustrates the result of the calculation for λ_r/ω_b as a function of solvent shear viscosity with a barrier frequency of $\omega_b = 9.6 \times 10^{12}$ s^{-1}, which is compared with the experimental result. The solid line in the figure represents the relation of $\lambda_r/\omega_b = A/(\eta)^\alpha$ with $\alpha = 0.40$. For comparison, the result predicted by Kramers theory for $\omega_b = 9.6 \times 10^{12}$ s^{-1} is shown in the same figure.

Nature of Potential Barrier. Application of the present frequency-dependent friction model provides information on the form of the potential barrier. Qualitatively, the value of ω_b can be regarded as describing the frequency motion accross a small but critical range of ϕ at the barrier top; i.e., at the barrier top ω_b can be written as

$$\omega_b = \{(|d^2U(\phi)/d\phi^2|)/I\}^{1/2} \tag{11}$$

where $U(\phi)$ is the intramolecular torsional potential.

From the torsional potential that has been obtained by Siegel et al.[22] for the S_1 state of 2VA by the semiempirical molecular orbital computation by using AM1 Hamiltonians, $\omega_b = (7.8-8.3) \times 10^{12}$ s^{-1} can be deduced. Here, the radius of the sphere corresponding to the van der Waals volume was used for the calculation of the I value in eq 11.

On the other hand, Barbara and co-workers[5] have determined the value of the barrier frequency of the S_1-state isomerization of 22PA and 2VA by simply estimating an effective torsional potential of the truncated form

$$2U(\phi) = V_1(1 - \cos\phi) + V_2(1 - \cos 2\phi) \tag{12}$$

where the parameters V_1 and V_2 have been determined from the experimentally obtained activation energies; $V_1 = E_a^f - E_a^r$ and $V_2 = E_a^f - V_1/2$. It is interesting to note that the resulting values of $\omega_b = 8.9 \times 10^{12}$ s^{-1} for 22PA and 15.6×10^{12} s^{-1} for 2VA are in excellent agreement with our results, although the methods of determination are quite different from each other.

Furthermore, by using the G−H transmission coefficient (λ_r/ω_b) determined in the present work (Figure 6), k_{TST} can be deduced separately. As a result, the ω_0 value is determined as 9.1×10^{12} s^{-1}, where 15.5 kJ/mol is taken as E_a.[5] We find that this is almost coincident with the ω_b value. It is not unphysical to assume that ω_b is comparable with ω_0. From the S_1-state torsional potential obtained from laser-induced fluorescence measurements, the ω_0 values are deduced as $\omega_0/(2\pi c) = 23.3$ cm^{-1} ($\omega_0 = 4.4 \times 10^{12}$ s^{-1}) for 2-phenylanthracene and $\omega_0/(2\pi c) = 66.8$ cm^{-1} ($\omega_0 = 13 \times 10^{12}$ s^{-1}) for 9-phenylanthracene.[23] These almost correspond to the present ω_b and ω_0 values.

In Table 1 the values of ω_b, E_a, and α of S_1-state 22PA isomerization are compared with those of S_1-state 2VA isomerization.[3,5,9] 22PA has smaller values for both ω_b and E_a than 2VA. This indicates that the 22PA isomerization has a flatter-topped lower potential barrier compared to the potential barrier for the 2VA isomerization. The ω_b value of 22PA is smaller by a factor of 1.2 than that of 2VA. This is caused by the difference in the *I* value in eq 11, which is due to the difference in size of the twisting moiety. The larger α value for 22PA is related to the lower barrier frequency (ω_b).

The ω_b values for the S_1-state isomerization of *trans*-stilbene and DPB are also included in Table 2 for comparison, which have been obtained by the solvent-changing method.[18,24] It has been concluded that these ω_b values are unphysically low for the top of the barrier to the isomerization. This criticism is based on the consideration that these ω_b values, which have been determined by the same method of calculation as in the present work, are too small compared to the frequency of the torsional motion about the ethylenic double bond, i.e., $\omega_b/(2\pi c) = 445-469$ cm^{-1} (i.e., $\omega_b = (83-88) \times 10^{12}$ cm^{-1}) calculated for the modes that include torsion about the double bond of the S_1-state of *trans*-stilbene.[25]

An interesting additional comparison can be made between the isomerizations in 2-alkenylanthracene and in diphenylpolyene. For 2-alkenylanthracene it is reasonable to consider that its potential barrier is considerably flatter than that of the torsional motion about the ethylenic double bond. This is due to the difference in the bond strengths between the single and double bonds. Therefore, a ω_b value significantly smaller than the frequency of the ethylene torsional motion cited above will be required for the isomerization of 2-alkenylanthracene.

Summary and Conclusions

The solvent shear-viscosity dependence of the excited S_1-state isomerization rate constant of 22PA has been determined by means of the high-pressure study of picosecond time-resolved fluorescence spectroscopy. The viscosity dependence can be described by the power-law formula with an exponent of $\alpha = 0.40$. The viscosity dependence of 22PA isomerization is appreciably greater than that of 2VA ($\alpha = 0.20$). This can be interpreted as due to the larger size of the twisting moiety in 22PA compared to the size in 2VA.

The α value indicates that the viscosity dependence is too weak for application of Kramers theory. The experimental results have been well explained by the frequency-dependent friction ($\zeta(\lambda_r)$), which is defined in the G−H theory. From the best fit, the frequency for the top of the potential barrier to the isomerization of 22PA, $\omega_b = 9.6 \times 10^{12}$ s^{-1}, has been shown to reproduce the experimental viscosity dependence. This ω_b value is considered to be a *realistic* value for the torsional motion around a single bond; i.e., it is concluded that with the present viscosity values ($\eta < 10$ mPa s), the frequency-dependent friction has been reasonably evaluated by *hydrodynamic theory* without introducing the *mode-coupling theory* whose contribution has recently been discussed by Bagchi[26] for slow and viscous liquid systems.

Finally, it should be stressed that the weak dynamic solvent effect as in the present system can only be determined accurately by the high-pressure method, which allows us to cover a wide viscosity range in a *single* solvent.

Acknowledgment. This work was supported in part by a Grant-in-Aid for Scientific Research (No. 06214213) from the Ministry of Education, Science, and Culture.

References and Notes

(1) See the following reviews. Hynes, J. T. In *Theory of Reaction Dynamics*; Baer, M., Ed.; CRC Press: Boca Raton, FL, 1985; Vol. IV, Chapter 4, p 171. Hänggi, P.; Talkner, P.; Borkovec, M. *Rev. Mod. Phys.* **1990**, *62*, 251, and references therein.

(2) Flom, S. R.; Brearley, A. M.; Kahlow, M. A.; Nagarajan, V.; Barbara, P. F. *J. Chem. Phys.* **1985**, *83*, 1993.

(3) Flom, S. R.; Nagarajan, V.; Barbara, P. F. *J. Phys. Chem.* **1986**, *90*, 2085.

(4) Brearley, A. M.; Flom, S. R.; Nagarajan, V.; Barbara, P. F. *J. Phys. Chem*. **1986**, *90*, 2092.

(5) Kang, T. J.; Etheridge, T.; Jarzeba, W.; Barbara, P. F. *J. Phys. Chem*. **1989**, *93*, 1876.

(6) Birks, J. B. *Chem. Phys. Lett*. **1978**, *54*, 430. Tavan, P.; Schulter, K. *Chem. Phys. Lett*. **1978**, *56*, 200.

(7) Hicks, J. M.; Vandersall, E. V.; Sitzmann; Eisenthal, K. B. *Chem. Phys. Lett.* **1987**, *135*, 413.

(8) Hara, K.; Kiyotani, H.; Kajimoto, O. *J. Chem. Phys.* **1995**, *103*, 5548.

(9) Hara, K.; Kiyotani, H.; Bulgarevich, D. S. *Chem. Phys. Lett.* **1995**, *242*, 455.

(10) Stolka, M.; Yanus, J. F.; Pearson, J. M. *Macromolecules* **1976**, *9*, 710.

(11) Hara, K.; Morishima, I. *Rev. Sci. Instrum.* **1988**, *59*, 2377.

(12) Hara, K.; Kometani, N.; Kajimoto, O. *Chem. Phys. Lett.* **1994**, *225*, 381.

(13) Bridgman, P. W. *Collected Experimental Papers*; Harvard University Press: Cambridge, MA, 1964; Vol. IV,

(14) $\eta = a + bP + cP^2 + dP^3$, where *a*, *b*, *c*, and *d* are numerical constants. We found that over the whole viscosity range examined, this relation reproduces the experimental data much better than the empirical relation $\eta = \eta_0 \exp(\gamma P)$, where η_0 is the viscosity at atmospheric pressure and γ is a constant.

(15) Bulgarevich, D. S.; Kajimoto, O.; Hara, K. *J. Phys. Chem*. **1995**, *99*, 13356.

(16) Kramers, H. A. *Physica* **1940**, *7*, 284.

(17) Grote, R. F.; Hynes, J. T. *J. Chem. Phys.* **1980**, *73*, 2715; **1981**, *74*, 4465.

(18) Rothenberger, G.; Negus, D. K.; Hochstrasser, R. M. *J. Chem. Phys.* **1983**, *79*, 5360.

(19) Bagchi, B.; Oxtoby, D. W. *J. Chem. Phys.* **1983**, *78*, 2735.

(20) Hawley, S.; Allegra, J.; Holton, G. *J. Acoust. Soc. Am.* **1970**, *47*, 137.

(21) Allegra, J.; Hawley, S.; Holton, J. *J. Acoust. Soc. Am.* **1970**, *47*, 144.

(22) Ni, Y.; Siegel, J. S.; Hsu, V. L.; Kearns, D. R. *J. Phys. Chem.* **1991**, *95*, 8211. Ni, Y.; Siegel, J. S.; Kearns, D. R. *J. Phys. Chem*. **1991**, *95*, 9208.

(23) Werst, D. W.; Brearley, A. M.; Gentry, W. R.; Barbara, P. F. *J. Am. Chem. Soc.* **1987**, *109*, 32.

(24) Velsko, S. P.; Fleming, G. R. *J. Chem. Phys.* **1983**, *76*, 3553.

(25) Warshel, A. *J. Chem. Phys.* **1975**, *62*, 214.

(26) Bagchi, B. *J. Chem. Phys.* **1996**, *105*, 7543